A Journal of the Gesellschaft Deutscher Chemiker

Angewandte International Edition GDCh Chemie

www.angewandte.org

Accepted Article

Title: Post-synthetic Rhodium (III) Complexes in Covalent Organic Frameworks for Photothermal Heterogeneous C-H Activation

Authors: Teng Li, Pei-Lin Zhang, Long-Zhang Dong, and Ya-Qian Lan

To be cited as: *Angew. Chem. Int. Ed.* **2024**, e202318180

Link to VoR: https://doi.org/10.1002/anie.202318180

WILEY VCH

10.1002/anie.202318180

WILEY VCH

RESEARCH ARTICLE

Post-synthetic Rhodium (III) Complexes in Covalent Organic Frameworks for Photothermal Heterogeneous C-H Activation

Teng Li, Pei-Lin Zhang, Long-Zhang Dong, Ya-Qian Lan*

[*] Dr. T. Li, P.-L. Zhang, Dr. L.-Z. Dong, Prof. Y.-Q. Lan
School of Chemistry
South China Normal University
Guangzhou, 510006 (P. R. China)
E-mail: yqlan@m.scnu.edu.cn

Supporting information for this article is given via a link at the end of the document.

Abstract: Although photocatalytic C-H activation has been realized by using heterogeneous catalysts, most of them require high-temperature conditions to provide the energy required for C-H bond breakage. The catalysts with photothermal conversion properties can catalyze this reaction efficiently at room temperature, but so far, these catalysts have been rarely developed. Here, we construct bifunctional catalysts Rh-COF-316 and -318 to combine photosensitive covalent organic frameworks (COFs) and transition-metal catalytic moiety using a post-synthetic approach. The Rh-COF enable the heterogeneous C-H activation reaction by photothermal conversion for the first time, and exhibit excellent yields (up to 98%) and broad scope of substrates in [4+2] annulation at room temperature, while maintaining the high stability and recyclability. Significantly, this work is the highest yield reported so far in porous materials catalyzing $C(sp^2)$-$C(sp^2)$ coupling at room temperature. The excellent performances can be attributed to the COF-316, which enhances the photothermal effect (ΔT = 50.9 °C), thus accelerating C-H bond activation and the exchange of catalyst with substrates.

Introduction

In recent years, transition-metal catalyzed C-H bond activation reactions have become sustainable and complementary methods to traditional synthetic processes, owing to their step- and atom-economical nature.[1] However, these reactions are often carried out at higher temperatures, and thus, recent research has focused on developing greener and more resource-economical approaches for achieving these reactions under mild reaction conditions.[2] Photocatalysis, which offers an atom-economically and environmentally friendly alternative, presents a milder alternative pathway to thermally driven reactions through the transfer of energy or electrons absorbed by light.[3] The combination of transition-metal catalysis and photocatalysis has become a multifunctional platform for the development of C-H activation.[4] Photocatalysis can assist the basic organometallic reaction step by modulating the oxidation state of the transition metal complex or by occurring the energy transfer to excite of the intermediate catalytic species.[5] However, most of these approaches rely heavily on the simultaneous addition of transition-metal catalyst and photosensitizer, which can be expensive and difficult to recycle (Scheme 1a).[6] Thus, it will be highly demanded to develop heterogeneous catalyst to fulfill the requirements of true green chemistry and industrial applications.

Covalent organic frameworks (COFs), a class of crystalline porous organic materials, are assembled with small organic molecules to form higher order structures.[7] Compared with traditional homogeneous catalysts, COFs have the following outstanding advantages, making them qualified as heterogeneous photocatalysts: (i) The organic small molecule building blocks of COFs facilitate the introduction of photosensitive groups, thus enabling the construction of multifunctional photocatalysts;[8] (ii) The porosity and large specific surface area of COFs contribute to enhance the catalytic activity and benefit the mass transfer of substrates, providing the possibility of new catalysis;[9] (iii) COFs connected by covalent bonds have good chemical and thermal stability, so that they remain stable in most reaction systems even under harsh conditions and allow for recycling and reusing after reaction;[10] (iv) The very strong π-π interactions and extended conjugate structure of COFs not only promote the separation, diffusion and migration of light-generated electron-hole pairs, but also enable efficient photothermal conversion;[11] (v) COFs can improve their photocatalytic activity or achieve multifunctional performances through post synthesis modification.[12] Therefore, COFs can provide an ideal powerful platform for heterogeneous photocatalysis. Currently, COFs in photocatalytic C-H activation reactions mainly involve cross-dehydrogenative coupling between tetrahydroisoquinoline derivatives and nucleophilic reagents, and alkylation reactions of aromatic compounds.[13] These reactions basically involve free radicals and single electron transfer courses, in which photosensitive COFs play a good role as electron transfer carriers.[14] However, in most of transition-metal catalyzed C-H activation, the reaction processes are not involved in the free radical course, but rather an organometallic step in which the C-H bond is cleaved to form C-M (M for metal) bond.[15] And the rate-determining step of the reactions depends on the breakage process of the highly thermodynamically stable C-H bonds (bond dissociation energy ≥ 90-110 kcal mol^{-1}). Therefore, it is necessary to develop a class of COFs materials that can generate photothermal effects to facilitate C-H bond breaking step and thus drive C-H activation reaction cycle.

10.1002/anie.202318180

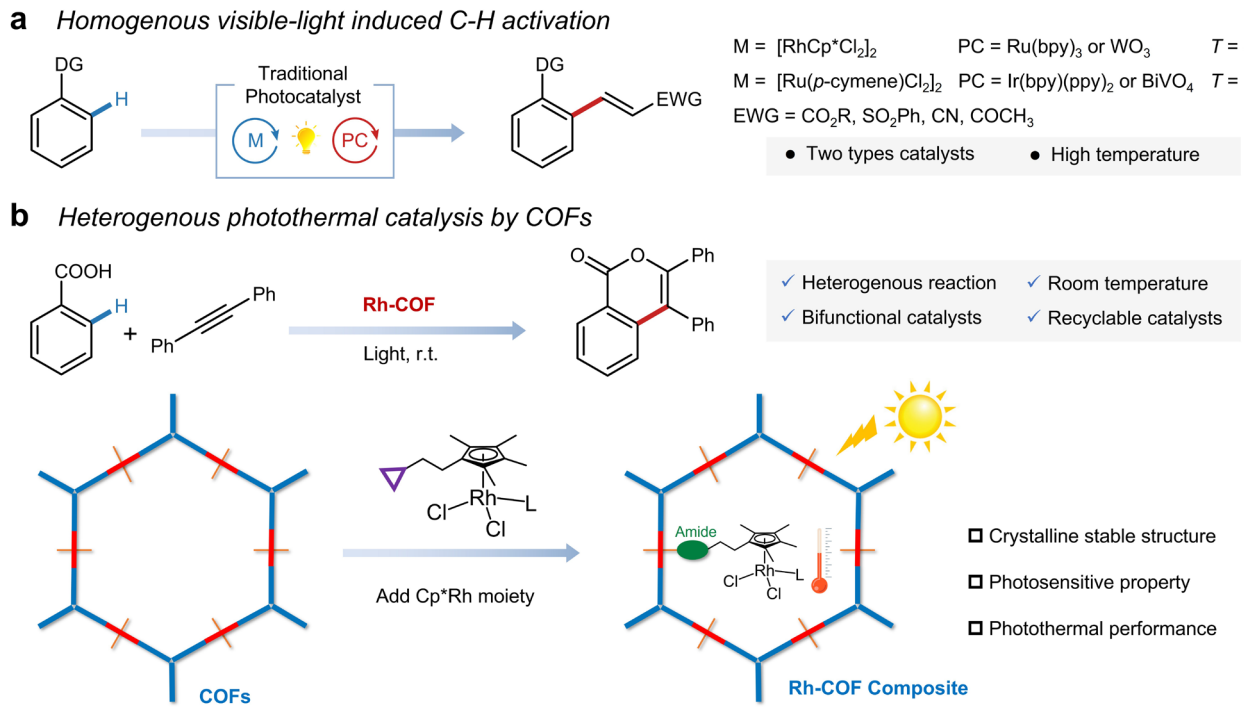

Scheme 1. Post-synthetic COFs by Rh moiety as heterogeneous photothermal catalyst for C-H annulation of aromatic acids with alkynes.

Herein, we report the design and synthesis of two COFs-based composites Rh-COF-316 and -318 for heterogeneous photothermal C-H activation reactions. Benefiting from the ordered structure of COFs and the covalent bond of the cyclopentadiene Rh^{III} block, the uniformly distributed Rh-COF are formed spontaneously by a programmable method according to the position of the reserved carboxyl groups in the COFs (Scheme 1b). The post-synthesized Rh-COF are used to catalyze the [4+2] annulation of benzenic with alkynes to product isocoumarins, an important class of pharmaceutical intermediates.[16] In contrast to homogenous catalytic C-H activations, the Rh-COF complexes in heterogeneous system simultaneously fulfill bifunctional roles. The first role is to absorb light and provide sufficient thermal energy (photothermal conversion efficiency ΔT = 50.9 °C) to the reaction center, while the second role is to enable efficient binding of reaction substrates and catalytic sites, as well as the rapid diffusion of products. With these advantages, the Rh-COF catalysts exhibit excellent product yield (up to 98%), wide range of substrates, high stability and good reusability.

Results and Discussion

We proposed a strategy to achieve heterogeneous C-H activation by post-synthetic strategy, enabling uniform loading of cyclopentadiene moiety in the COFs. The Rh-COF-316/318 complexes were synthesized by the model condensation reaction of 2,3,6,7,10,11-hexahydroxytriphenylene (HHTP), tetrafluorophthalonitrile (TFPN) or 2,3,5,6-tetrafluoro4-pyridinecarbonitrile (TFPC), and the amidation reaction of $[(\mu^5\text{-}Me_4Cp(CH_2)_2NH_3)RhCl_2]_2Cl_2$ (Rh moiety) (Figure 1a). Inductively coupled plasma mass spectrometry (ICP-MS) confirmed the successful preparation of Rh-COF-316 and -318 with average Rh contents of about 7.68±0.3 and 7.05±0.3 wt.%, respectively, indicating the presence of about one Rh molecule per unit cell. To investigate the structure of the obtained complexes, powder X-ray diffraction (PXRD) was used. It is remarkable that the crystallinity of Rh-COF complexes was preserved despite the post-synthesis reaction process. The characteristic diffraction peaks observed in these complexes were attributed to COF-316 and -318 without obvious shifts compared to the pre-synthesis state (Figure 1b, S1). Based on the above results, it is determined that the density of the post-synthesis catalytic sites was at a low level, and the effect of spatial resistance and framework structure induced the existence of sufficient space between them to facilitate the catalytic reaction (Figure 1c).

Furthermore, the fourier transform infrared (FT-IR) spectrums confirmed the successful formation of amide bonds between the initial COFs and the cyclopentadiene block. The spectrum exhibited a strong amide C=O stretching peak at 1642 cm^{-1}, while the original C-N peak of COF-316 and -318 at 2240 cm^{-1} and the C=O peak of COF-COOH at 1717 cm^{-1} disappeared, indicating the reduction of the initial COFs and their linkage to the cyclopentadiene block by amide bonds (Figure 2a, S2-3). To further confirm the C=O stretching peak, we synthesized two small molecule fragments of Rh-COF. The FT-IR spectra showed the amide C=O stretching mode at 1645 cm^{-1} (Figure S4), which is consistent with the measurements of Rh-COF. The formation of amide bonds was confirmed by ^{13}C cross-polarization magic angle spinning (CP-MAS) NMR spectroscopy (Figure 2b and S5). By comparing COF-316/318 and free Rh moiety, the peak at ~ 163 ppm was assigned to the generated amide group, while the peaks

10.1002/anie.202318180

RESEARCH ARTICLE

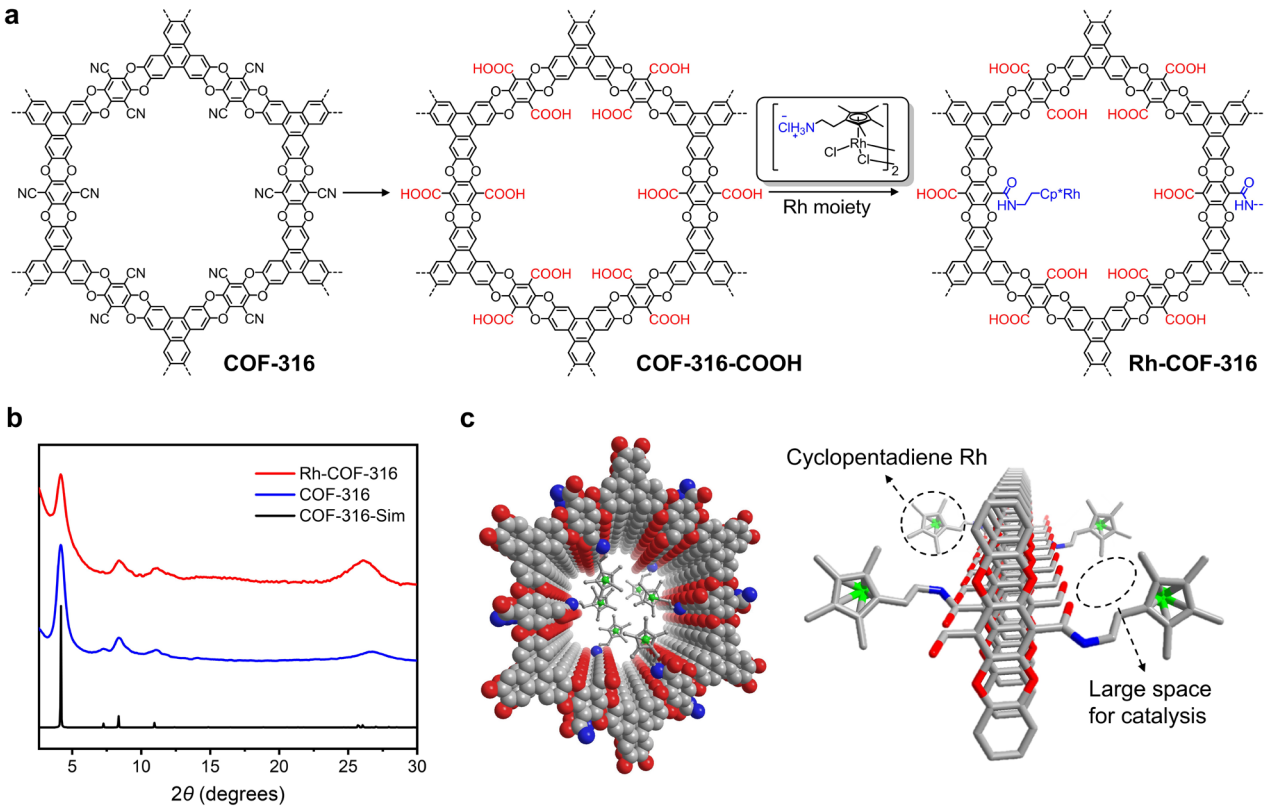

Figure 1. (a) Synthesis of Rh-COF-316 via post-synthesis with Rh moiety followed by amidation reaction. (b) The PXRD patterns of COF-316-simulation, COF-316 and Rh-COF-316. (c) The schematic diagrams of the arrangement of cyclopentadienylrhodium in the channel structure.

below 50 ppm were assigned to the the cyclopentadiene compound (Figure S6).[17] In addition, all these chemical shifts in Rh-COF aligned closely with those of the corresponding small molecule fragments (Figure S7-8). Then, the X-ray photoelectron spectroscopy (XPS) analysis was performed. The deconvolution N 1s XPS spectra of Rh-COF and Rh moiety showed a significant shift in binding energy after post-synthesis. (Figure 2c). [18] The XPS results of the other elements can be found in Figure S9. The above results illustrated that the cyclopentadiene moiety was successfully connected to COFs by amide bond. The thermal stability of Rh-COF-316 and -318 were verified by thermogravimetric analysis (TGA). Both COFs complexes exhibited good thermal stability (up to 200 °C, Figure S11-14), which satisfied the need for potential applications in catalysis. In contrast to the TGA of COF-316 and -318. The BET surface areas were investigated by N_2 adsorption-desorption isotherm at 77 K (Figure S15-16). The surface areas of COF-316-Rh and 318-Rh were 68 and 15 m^2g^{-1}, respectively. Compared to the original COF-316 and -318, the noticeable decline in the surface areas indicated that the coordination of Rh moiety enhanced the weight of COFs significantly. Nevertheless, the thermal stability and BET surface area were still sufficient for the catalytic applications.

Then, the UV-Vis diffuse reflectance spectra of Rh-COF-316 and -318 were performed. Strong absorption peaks in the range of 200-500 nm were observed, which was in good agreement with the performance of the original COFs (Figure 2d, S17). This results indicated that the optical activity of the constructed Rh-COF was mainly derived from their incorporated COFs. The layer structures of Rh-COF-316 and -318 were characterized by scanning electron microscopy (SEM) and transmission electron microscopy (TEM). The SEM images showed that both complexes clearly revealed the layered-sheet morphology (Figure 2e, S18). After post-synthesis the layer structure was not destroyed and remained unchanged, which was attributed to the stable COFs crystalline structure and mild chemical modification means. Energy dispersive spectroscopy (EDS) elemental mapping images clearly showed that the Rh, N and Cl elements were uniformly distributed in the structure of the Rh-COF complex (Figure 2f, S19). Meanwhile, we observed the microscopic morphology of Rh-COF-316/318 by high-resolution transmission electron microscopy (HRTEM) (Figure S20-21). The successful achievement of uniformly distributed catalytic species of cyclopentadiene Rh composites within the COFs using our designed post-synthesis approach confirmed the versatility of this method. For heterogeneous photocatalysts, the photo absorption capacity of the catalyst was very important. In general, the post-synthetic Rh-COF should be very promising catalysts for heterogeneous photocatalytic reactions.

C-H activation, known for its step- and atomic-economy, has been emerged as a powerful approach for synthesizing important natural and bioactive compounds. Traditionally, C-H activation

10.1002/anie.202318180

WILEY VCH

RESEARCH ARTICLE

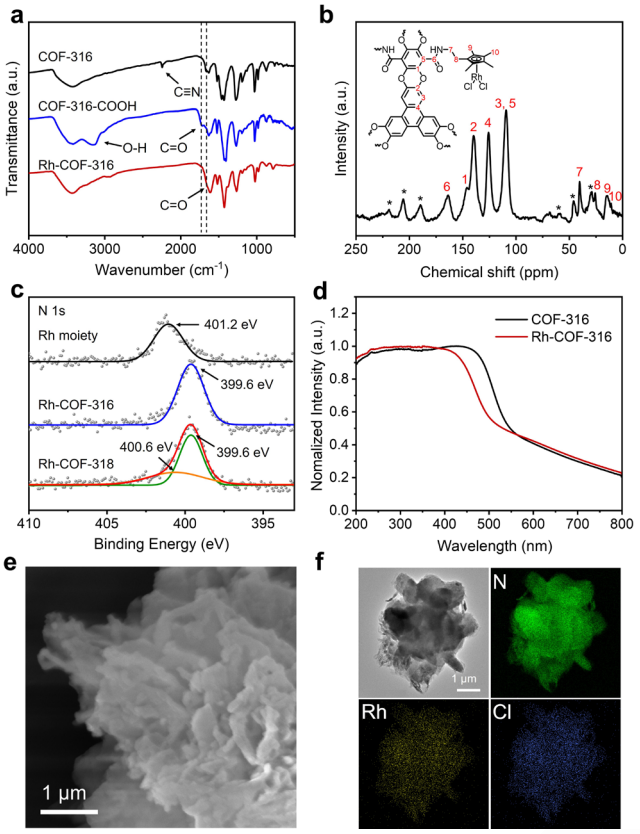

Figure 2. (a) The FT-IR of COF-316, COF-316-COOH and Rh-COF-316. (b) Solid ^{13}C NMR spectra of Rh-COF-316. (c) The deconvoluted N 1s XPS spectra of Rh moiety, Rh-COF-316 and Rh-COF-318. (d) Solid-state reflectance UV-vis spectra of COF-316 and Rh-COF-316. The SEM image (e) and EDS mapping images (f) of Rh-COF-316.

reactions were carried out under thermocatalytic conditions. However, the use of photocatalysis offered distinct advantages in terms of environmental sustainability and economic viability. Rh-COF-316 and -318, possessing both photoactivity and transition metal catalytic activity, enabled C-H activation under xenon lamp.

To investigate the photo-driven catalytic activity, the Rh-COF-316 and -318 were employed as heterogeneous catalyst for [4+2] annulation of benzoic and alkynes, which was commonly C-H activation accomplished by homogeneous catalysts under high temperature.[19] We began the study by the model reaction of benzoic acid (**1a**) and diphenylacetylene (**2a**) in MeOH with $Cu(OAc)_2·H_2O$ (1.0 equiv) and AgOAc (1.0 equiv) as the additive at room temperature under xenon lamp irradiation with the full spectrum. In which $Cu(OAc)_2$ was used as oxidizing agent, while AgOAc was used as a reagent to remove chlorine from the catalyst. In the presence of 10 mg COF-316-Rh, isocoumarin **3a** was produced with trace yield. When many green solvents were screened, the product was essentially not generated (Table S1, entry 1-6). To our delight, **3a** was formed with 95% yield in dichloroethane (DCE) (Table S1, entry 7). A screen of additives shows that both $Cu(OAc)_2·H_2O$ and AgOAc were required, a single additive would give a very small amount of product (Table S1, entry 8-9). Interestingly, when the catalyst was switched from Rh-COF-316 to Rh-COF-318, product **3a** was also obtained 83%

Table 1. Substrate scope of the C-H annulation of aromatic acids and alkynes.[a]

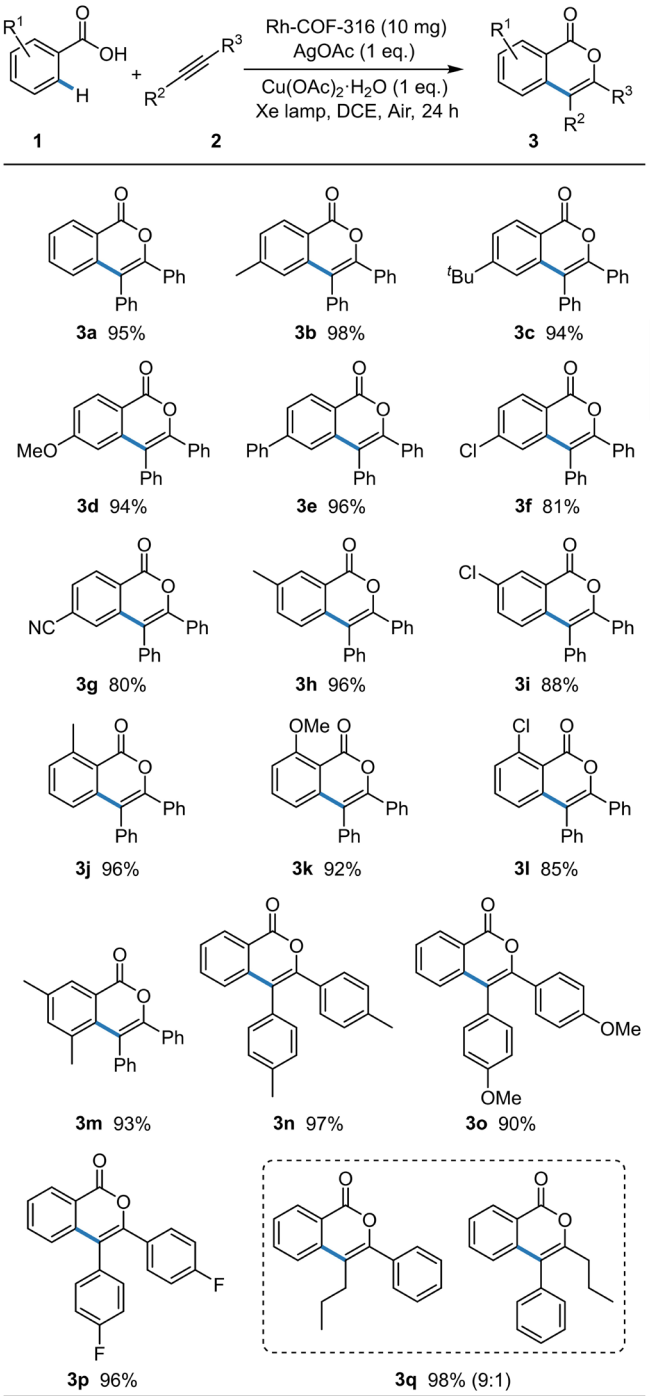

[a] Reaction condition: **1** (0.10 mmol, 1.0 equiv), **2** (1.2 equiv), Rh-COF-316 (10 mg), AgOAc (1.0 equiv), xenon lamp, $Cu(OAc)_2·H_2O$ (1.0 equiv), DCE (1.0 mL), under air for 24 h at room temperature. Cited yields were the isolated yields. Ratio of regioisomers were determined by ^1H NMR.

yield (Table S1, entry 10). The result indicated that the post-synthetic method could be generalized to obtain highly active heterogeneous catalysts, and the subtle variation in catalytic performance might be due to the differences in the loading of Rh moiety and COFs structure. The desired [4+2] annulation could not proceed without COF-316 or Rh moiety loading (Table S1,

10.1002/anie.202318180

entry 11-12), which indicated that the Rh-COF complexes catalysts exhibited dual-functional heterogeneous catalytic activity by coupling Rh moiety. Two small molecule fragments of Rh-COF were likewise tried, and it was shown that neither of them catalyzed the reaction very well (Table S1, entry 13-14). When the reaction was carried out under a dark environment at room temperature, **3a** was significantly reduced to trace yield (Table S1, entry 15). By using 5 mg Rh-COF-316, the yield decreased to 60% (Table S1, entry 16). When switching to pure oxygen, the yield dropped to 92% due to a side reaction in which the **2a** substrate was partially oxidized (Table S1, entry 17). In the case of pure oxygen without $Cu(OAc)_2 \cdot H_2O$, no product was obtained (Table S1, entry 18), which indicated that oxygen could not be used as an oxidant in C-H activation reaction and was detrimental to the reaction. When the reaction was carried out under nitrogen, the yield of **3a** was still 95%, which was the same as the yield in air (Table S1, entry 19). Therefore, the effect of oxygen in air was limited, and we finally chose to carry out the reaction in air. Decreasing the additive loading would further decline the yield (Table S1, entry 20 and 21). Moreover, the reaction also maintained a similar catalytic efficiency under thermal condition (Table S1, entry 22).

Subsequently, the functional group tolerance and substrate scope were investigated with respect to the heterogeneous photo-driven thermocatalysis of isocoumarin (Table 1). Annulations with diphenylacetylene **2a** and benzoic acids **1** bearing electron-donating and electron-withdrawing *para*-substituents progressed smoothly with good yield (80-98%) to give corresponding products (**3a-3g**). It is noteworthy that the substrate with a functional group such as cyanide (**3g**) was also compatible with this reaction condition. Meanwhile, the *ortho*- and *meta*-substituted benzoic acids were also well tolerated and converted to the target products (**3h-3m**) with excellent yield (85-96%). Then, substituted alkynes **2** were examined with benzoic acid **1a**. For moderately coordinating alkynes, the reactions occurred with excellent yield (90-97%) to afford product **3n-3p**. With respect to the unsymmetrical alkyne, the substrate with alkyl chain on one side and aryl group on the other was also smoothly transformed into the target product **3q** in outstanding yield (98%) and good regioselectivity (9:1).

To exclude the effect of free Rh moiety, we carried out control experiments with the standard condition in the absence of substrates. The mixture with Rh-COF-316 was stirred under xenon lamp for 24 h, and the filtrate obtained by filtration was used to catalyze the reaction of benzoic acid **1a** and diphenylacetylene **2a**. As expected, the reaction could not proceed to obtain the desired product. According to the Rh content in the filtrate measured by ICP analysis, just only less than 0.05% Rh corresponding to 0.0033 wt% Rh content in Rh-COF-316 was present in the filtrate. Similarly, it has been shown in the previous condition screening that the single Rh block cannot catalyze the reaction (Table S1, entry 12). We also performed EDS analysis on the reacted Rh-COF-316, and the results showed that the Rh element remained evenly distributed in the complex with the original loading (Figure S22). These results imply that the Rh moiety was tightly linked to the COFs through covalent bonds, and only trace amounts of Rh were isolated without catalytic effect

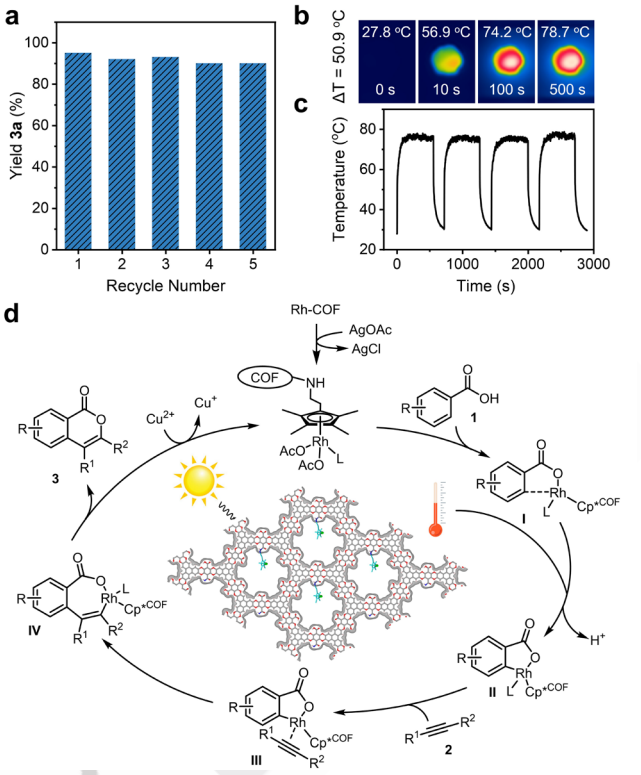

Figure 3. (a) The recycle catalytic reaction by used Rh-COF-316. (b) Photothermal images of Rh-COF-316 under different light times. (c) Cycling tests of temperature changes of Rh-COF-316 under irradiation. (d) Proposed reaction mechanism.

under the reaction conditions.

For photo-driven organic transformations in heterogeneous system, the catalyst recycling was an important indicator to satisfy industrial application. Rh-COF-316 was further examined to reused for several times in the standard condition, the activity and selectivity were maintained at least for five cycles followed by excellent yield of **3a** (Figure 3a). The PXRD patterns of the recycled Rh-COF-316 showed that the atomic-level structure was still maintained, despite the significant decrease in intensity of PXRD patterns (Figure S23). The decline of structural regularity was most likely due to the residue of other metal ions in the interlayer or pore during the repeated redox process of the catalyst. The Rh_{3d} XPS spectra indicated that the Rh was remained in its original state in recycled Rh-COF-316 (Figure S10). From the reaction rate, the number of cycles had no effect on the initial reaction rate, and the decrease of yield in the final reaction might be due to the loss of catalyst during the separation of the catalyst from the reaction system (Figure S24). It was also to be mentioned that each catalytic cycle required the addition of the stoichiometric amounts of Cu and Ag acetates.

In order to evaluate the performance of Rh-COF-316 in C-H activation reactions, we compared the performances of porous materials such as MOFs, COFs and amorphous porous organic polymers (POPs) as heterogeneous catalysts in $C(sp^2)$-$C(sp^2)$ bond formation (Figure S25). To date, our catalysts are the highest yielding $C(sp^2)$-$C(sp^2)$ formation in porous materials at

room temperature, and have a wide range of substrate applicability and recycling property.[20] In general, the Rh-COF prepared by our post-synthesis strategy not only have stable crystalline structure and photothermal properties, but also can achieve an efficient heterogeneous C-H activation reaction with excellent yield, selectivity and reproducible catalytic properties under mild conditions.

To explain the catalysis mechanism of photocatalytic cycle with Rh-COF-316, the control experiments were conducted. The optimization of reaction conditions revealed that the xenon light irradiation and acetate additions were necessary conditions to obtain high yield (Table S1). In particular, the increase of oxygen would instead reduce the object product, while the nitrogen atmosphere had no effect on the reaction, indicating that O_2 was not involved in the catalytic cycle of [4+2] annulation.

Therefore, we suggested that COFs played the role of light-promoted thermal catalysis to provide the required energy for C-H activation reaction. Evaluating the photothermal conversion performance of Rh-COF-316 by monitoring the temperature variation of the catalyst surface under light irradiation. After light exposure, the temperature difference (ΔT) can be as high as 50.9 °C (Figure 3b). Cyclic light experiments showed that the catalyst had excellent photothermal stability, and the maximum surface temperature remained essentially constant (Figure 3c). By comparing the light absorption and photothermal conversion performances, we can conclude that the photothermal performance of Rh-COF-316 was mainly contributed to the original COF-316, which can effectively achieve photothermal conversion due to the extended conjugated structure (Figure 2d and S26).[21] Accordingly, the heterogeneous Rh-COF-316 in reaction mixture provided a high-temperature microenvironment around the Rh catalytic site to supply the catalytic reaction cycle. Furthermore, Rh-COF-316 demonstrated the ability to produce the product in high yield at 60 °C without light (Table S1, entry 22), providing further evidence for the significance of light-promoted thermocatalytic C-H activation in this reaction. The deuterium-labeling experiment was conducted to further insight into the C-H activation mechanism (Figure S27). **1a**-d_5 was prepared in standard condition without diphenylacetylene **2a**. There were very few H/D exchange (< 1%) found in *ortho* position, suggesting that the initial cyclization realized by C-H bond cleavage was irreversible. In a competitive side-by-side reactions with **1a** and **1a**-d_5, the kinetic isotopic effect (KIE) of 2.1 was observed (Figure S28). It suggests that the C-H activation step was the rate-determining step in the reaction cycle.

According to the above mechanistic studies and previous reports,[22] a plausible catalytic cycle mechanism was proposed (Figure 3d). Firstly, Rh-COF-316 and AgOAc produced the Rh^{III} catalytic species, which reacted with **1** to give rhodium benzoate **I**. Then, the photothermal conversion and the coordination of the oxygen atom in carboxyl group of Rh-COF-316 can assist C-H bond cleavage, resulting in the five-membered rhodacycle **II**. This process possibly undergoes the concerted metalation-deprotonation (CMD) path under xenon lamp irradiation through the thermal effect of photoexcited COF part. Regioselective coordination and migratory insertion of alkyne **2** furnished the seven-membered rhodacycle **IV**, which produces the desired product **3** by reductive elimination. Finally, the reoxidation step of Rh^{I} by Cu^{II} to the Rh^{III} catalytic species keeps the catalytic cycle going.

Conclusion

In conclusion, we have successfully developed two Rh-COF complexes, Rh-COF-316 and -318, using a simple post-synthesis strategy and applied them to the photothermal catalytic heterogeneous C-H activation reaction. The porous two-dimensional layer structure together with the carboxylic acid group render the COF materials as an ideal framework to connect the Rh moiety. The synthesized Rh-COF-316 and -318, featuring a cyclopentadienylrhodium unit connected by a simple amidation reaction, are employed to the photocatalysis of the [4+2] annulation reaction. Owing to their stable crystalline structure, good photosensitivity, uniformly distributed Rh catalytic centers and inherent photothermal nature, the Rh-COF catalysts exhibit remarkable product yields up to 98%, broad scope of substrates, and high stability with good reusability. This is the first time to utilize the photothermal conversion properties of COFs materials to achieve photocatalytic heterogeneous C-H activation reaction. Significantly, the Rh-COF complexes exhibit highest yields of $C(sp^2)$-$C(sp^2)$ coupling compared to other porous materials under mild reaction condition due to their uniformly distributed structure and efficient photothermal conversion properties. The unique structure facilitates efficient access to the catalytic site and rapid mass transport of organic substrates, while the photosensitivity COFs produces a strong photothermal effect (ΔT= 50.9 °C), enhancing the overall reaction kinetic. This not only expands the application of COFs-based complexes in photocatalytic C-H activation reactions, but also validates the versatility and feasibility of obtaining heterogeneous catalysts through the post-synthesis combination of transition-metal building blocks. Therefore, we convince that our strategy will promote the utilization of functional COFs material for heterogeneous catalysis and potentially facilitate their industrial applications.

Acknowledgements

This work was financially supported by the NSFC (grants No. 22225109, 22071109, 22301083; 22301085), and the China Postdoctoral Science Foundation (No. 2021M701269). We thank Dr. Miao Xiong for help with photothermal measurements and draft correction.

Conflict of Interest

The authors declare no conflict of interest.

Keywords: Post-synthetic COFs • Photothermal Catalysis • Heterogeneous • C-H Activation • Rh Complex

[1] a) N. Goswami, T. Bhattacharya, D. Maiti, *Nat. Rev. Chem.* **2021**, *5*, 646–659; b) T. Rogge, N. Kaplaneris, N. Chatani, J. Kim, S. Chang, B. Punji, L. L. Schafer, D. G. Musaev, J. Wencel-Delord, C. A. Roberts, R. Sarpong, Z. E. Wilson, M. A. Brimble, M. J. Johansson, L. Ackermann, *Nat. Rev. Methods Primer* **2021**, *1*, 43; c) Y. He, Z. Huang, K. Wu, J. Ma, Y.-G. Zhou, Z. Yu, *Chem. Soc. Rev.* **2022**, *51*, 2759–2852.

[2] R. A. Sheldon, *Green Chem.* **2017**, *19*, 18–43.

[3] a) M. D. Kärkäs, J. A. Jr. Porco, C. R. J. Stephenson, *Chem. Rev.* **2016**, *116*, 9683–9747; b) N. A. Romero, D. A. Nicewicz, *Chem. Rev.* **2016**, *116*, 10075–10166.

[4] a) D. C. Fabry, M. Rueping, *Acc. Chem. Res.* **2016**, *49*, 1969–1979; b) J. Twilton, C. (Chip) Le, P. Zhang, M. H. Shaw, R. W. Evans, D. W. C. MacMillan, *Nat. Rev. Chem.* **2017**, *1*, 1–19; c) K. P. S. Cheung, S. Sarkar, V. Gevorgyan, *Chem. Rev.* **2022**, *122*, 1543–1625.

[5] a) J. C. Tellis, D. N. Primer, G. A. Molander, *Science* **2014**, *345*, 433–436; b) Z. Zuo, D. T. Ahneman, L. Chu, J. A. Terrett, A. G. Doyle, D. W. C. MacMillan, *Science* **2014**, *345*, 437–440; c) I. B. Perry, T. F. Brewer, P. J. Sarver, D. M. Schultz, D. A. DiRocco, D. W. C. MacMillan, *Nature* **2018**, *560*, 70–75.

[6] a) D. C. Fabry, J. Zoller, S. Raja, M. Rueping, *Angew. Chem. Int. Ed.* **2014**, *53*, 10228–10231; b) D. C. Fabry, M. A. Ronge, J. Zoller, M. Rueping, *Angew. Chem. Int. Ed.* **2015**, *54*, 2801–2805; c) D. C. Fabry, J. Zoller, M. Rueping, *Org. Chem. Front.* **2019**, *6*, 2635–2639.

[7] a) A. P. Côté, A. I. Benin, N. W. Ockwig, M. O'Keeffe, A. J. Matzger, O. M. Yaghi, *Science* **2005**, *310*, 1166–1170; b) H. M. El-Kaderi, J. R. Hunt, J. L. Mendoza-Cortés, A. P. Côté, R. E. Taylor, M. O'Keeffe, O. M. Yaghi, *Science* **2007**, *316*, 268–272; c) X. Guan, F. Chen, Q. Fang, S. Qiu, *Chem. Soc. Rev.* **2020**, *49*, 1357–1384.

[8] T. Zhang, G. Zhang, L. Chen, *Acc. Chem. Res.* **2022**, *55*, 795–808.

[9] M. Lu, M. Zhang, J. Liu, Y. Chen, J.-P. Liao, M.-Y. Yang, Y.-P. Cai, S.-L. Li, Y.-Q. Lan, *Angew. Chem. Int. Ed.* **2022**, *61*, e202200003.

[10] X. Guan, Q. Fang, Y. Yan, S. Qiu, *Acc. Chem. Res.* **2022**, *55*, 1912–1927.

[11] L. Yang, J. Wang, K. Zhao, Z. Fang, H. Qiao, L. Zhai, L. Mi, *ChemPlusChem* **2022**, *87*, e202200281.

[12] S. Liu, M. Wang, Y. He, Q. Cheng, T. Qian, C. Yan, *Coord. Chem. Rev.* **2023**, *475*, 214882.

[13] a) A. López-Magano, B. Ortín-Rubio, I. Imaz, D. Maspoch, J. Alemán, R. Mas-Ballesté, *ACS Catal.* **2021**, *11*, 12344–12354; b) H. Chen, W. Liu, A. Laemont, C. Krishnaraj, X. Feng, F. Rohman, M. Meledina, Q. Zhang, R. Van Deun, K. Leus, P. Van Der Voort, *Angew. Chem. Int. Ed.* **2021**, *60*, 10820–10827; c) W. Dong, Y. Yang, Y. Xiang, S. Wang, P. Wang, J. Hu, L. Rao, H. Chen, *Green Chem.* **2021**, *23*, 5797–5805.

[14] a) J. Jia, X. Bu, X. Yang, *J. Mater. Chem. A* **2022**, *10*, 11514–11523; b) S. Li, L. Li, Y. Li, L. Dai, C. Liu, Y. Liu, J. Li, J. Lv, P. Li, B. Wang, *ACS Catal.* **2020**, *10*, 8717–8726; c) T.-X. Luan, L. Du, J.-R. Wang, K. Li, Q. Zhang, P.-Z. Li, Y. Zhao, *ACS Nano* **2022**, *16*, 21565–21575.

[15] a) L. Yang, H. Huang, *Chem. Rev.* **2015**, *115*, 3468–3517; b) S. Jeong, J. M. Joo, *Acc. Chem. Res.* **2021**, *54*, 4518–4529.

[16] X. Wang, D. E. Wedge, S. J. Cutler, *Nat. Prod. Commun.* **2016**, *11*, 1934578X1601101.

[17] a) T. Reiner, D. Jantke, A. Raba, A. N. Marziale, J. Eppinger, *J. Organomet. Chem.* **2009**, *694*, 1934–1937. b) B. Zhang, M. Wei, H. Mao, X. Pei, S. A. Alshmimri, J. A. Reimer, O. M. Yaghi, *J. Am. Chem. Soc.* **2018**, *140*, 12715–12719.

[18] B. Sánchez-Page, M. V. Jiménez, J. J. Pérez-Torrente, V. Passarelli, J. Blasco, G. Subias, M. Granda, P. Álvarez, *ACS Appl. Nano Mater.* **2020**, *3*, 1640–1655.

[19] I. Choi, A. M. Messinis, X. Hou, L. Ackermann, *Angew. Chem. Int. Ed.* **2021**, *60*, 27005–27012.

[20] a) T.-H. Park, A. J. Hickman, K. Koh, S. Martin, A. G. Wong-Foy, M. S. Sanford, A. J. Matzger, *J. Am. Chem. Soc.* **2011**, *133*, 20138–20141; b) Y. Huang, T. Ma, P. Huang, D. Wu, Z. Lin, R. Cao, *ChemCatChem* **2013**, *5*, 1877–1883; c) H. T. N. Le, T. T. Nguyen, P. H. L. Vu, T. Truong, N. T. S. Phan, *J. Mol. Catal. Chem.* **2014**, *391*, 74–82; d) P. Pachfule, M. K. Panda, S. Kandambeth, S. M. Shivaprasad, D. D. Díaz, R. Banerjee, *J. Mater. Chem. A* **2014**, *2*, 7944–7952; e) N. T. S. Phan, C. K. Nguyen, T. T. Nguyen, T. Truong, *Catal. Sci. Technol.* **2014**, *4*, 369–377; f) C. Huang, J. Wu, C. Song, R. Ding, Y. Qiao, H. Hou, J. Chang, Y. Fan, *Chem. Commun.* **2015**, *51*, 10353–10356; g) Y.-B. Huang, M. Shen, X. Wang, P. Huang, R. Chen, Z.-J. Lin, R. Cao, *J. Catal.* **2016**, *333*, 1–7; h) N. B. Nguyen, G. H. Dang, D. T. Le, T. Truong, N. T. S. Phan, *ChemPlusChem* **2016**, *81*, 361–369; i) H. T. T. Nguyen, D. N. A. Doan, T. Truong, *J. Mol. Catal. Chem.* **2017**, *426*, 141–149; j) S. Liu, W. Pan, S. Wu, X. Bu, S. Xin, J. Yu, H. Xu, X. Yang, *Green Chem.* **2019**, *21*, 2905–2910; k) K. Otake, J. Ye, M. Mandal, T. Islamoglu, C. T. Buru, J. T. Hupp, M. Delferro, D. G. Truhlar, C. J. Cramer, O. K. Farha, *ACS Catal.* **2019**, *9*, 5383–5390; l) I. Anastasiou, N. Van Velthoven, E. Tomarelli, A. Lombi, D. Lanari, P. Liu, S. Bals, D. E. De Vos, L. Vaccaro, *ChemSusChem* **2020**, *13*, 2786–2791; m) N. Huber, K. A. I. Zhang, *Eur. Polym. J.* **2020**, *140*, 110060; n) Z. Li, S. Han, C. Li, P. Shao, H. Xia, H. Li, X. Chen, X. Feng, X. Liu, *J. Mater. Chem. A* **2020**, *8*, 8706–8715; o) M. Tian, S. Liu, X. Bu, J. Yu, X. Yang, *Chem. – Eur. J.* **2020**, *26*, 369–373; p) N. Van Velthoven, Y. Wang, H. Van Hees, M. Henrion, A. L. Bugaev, G. Gracy, K. Amro, A. V. Soldatov, J. G. Alauzun, P. H. Mutin, D. E. De Vos, *ACS Appl. Mater. Interfaces* **2020**, *12*, 47457–47466; q) H. Cheng, C. Zang, F. Bian, Y. Jiang, L. Yang, F. Dong, H. Jiang, *Catal. Sci. Technol.* **2021**, *11*, 5543–5552; r) Y. Mohr, M. Alves-Favaro, R. Rajapaksha, G. Hisler, A. Ranscht, P. Samanta, C. Lorentz, M. Duguet, C. Mellot-Draznieks, E. A. Quadrelli, F. M. Wisser, J. Canivet, *ACS Catal.* **2021**, *11*, 3507–3515; s) Y. Tang, F. Chen, S. Wang, Q. Sun, X. Meng, F.-S. Xiao, *Chem. – Eur. J.* **2021**, *27*, 8684–8688; t) Y. Tang, Z. Dai, S. Wang, F. Chen, X. Meng, F.-S. Xiao, *Chem. – Asian J.* **2021**, *16*, 2469–2474.

[21] a) S. Liu, Z. Liu, Q. Meng, C. Chen, M. Pang, *ACS Appl. Mater. Interfaces* **2021**, *13*, 56873–56880; b) D. Dutta, J. Wang, X. Li, Q. Zhou, Z. Ge, *Small* **2022**, *18*, 2202369; c) Y.-R. Wang, H.-M. Ding, S.-N. Sun, J. Shi, Yi.-L. Yang, Q. Li, Y. Chen, S.-L. Li, Y.-Q. Lan, *Angew. Chem. Int. Ed.* **2022**, *61*, e202212162.

[22] K. Ueura, T. Satoh, M. Miura, *Org. Lett.* **2007**, *9*, 1407–1409.

10.1002/anie.202318180

RESEARCH ARTICLE

Entry for the Table of Contents

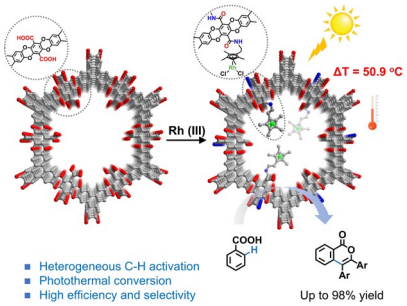

In this work, a general post-synthetic strategy for constructing bifunctional catalysts, Rh-COF, which connect photosensitive covalent organic frameworks and transition-metal catalytic groups through covalent bonding, was developed. Fascinatingly, such complexes enable efficient photothermal conversion properties, which can improve the photothermal catalytic performances in C-H activation to obtain excellent yield, substrate suitability and recyclability.